Quaternary Science Reviews 29 (2010) 2996–3005

Contents lists available at ScienceDirect

Quaternary Science Reviews

journal homepage: www.elsevier.com/locate/quascirev

Orbital- and millennial-scale changes in the hydrologic cycle and vegetation in the western African Sahel: insights from individual plant wax δD and δ^{13}C

Eva M. Niedermeyer [a,b,*], Enno Schefuß [a], Alex L. Sessions [b], Stefan Mulitza [a], Gesine Mollenhauer [a,c,d], Michael Schulz [a,c], Gerold Wefer [a,c]

[a] MARUM–Center for Marine Environmental Sciences, University of Bremen, P.O. Box 330 440, D-28334 Bremen, Germany
[b] California Institute of Technology, Department of Geological and Planetary Sciences, 17 Mail Stop 100-23, Pasadena, CA 91125, USA
[c] Department of Geosciences, University of Bremen, P.O. Box 330 440, D-28334 Bremen, Germany
[d] Alfred Wegener Institute, Am Handelshafen 12, D-27570 Bremerhaven, Germany

ARTICLE INFO

Article history:
Received 11 September 2009
Received in revised form
24 June 2010
Accepted 25 June 2010

ABSTRACT

To reconstruct variability of the West African monsoon and associated vegetation changes on precessional and millennial time scales, we analyzed a marine sediment core from the continental slope off Senegal spanning the past 44,000 years (44 ka). We used the stable hydrogen isotopic composition (δD) of individual terrestrial plant wax *n*-alkanes as a proxy for past rainfall variability. The abundance and stable carbon isotopic composition (δ^{13}C) of the same compounds were analyzed to assess changes in vegetation composition (C_3/C_4 plants) and density. The δD record reveals two wet periods that coincide with local maximum summer insolation from 38 to 28 ka and 15 to 4 ka and that are separated by a less wet period during minimum summer insolation. Our data indicate that rainfall intensity during the rainy season throughout both wet humid periods was similar, whereas the length of the rainy season was presumably shorter during the last glacial than during the Holocene. Additional dry intervals are identified that coincide with North Atlantic Heinrich stadials and the Younger Dryas interval, indicating that the West African monsoon over tropical northwest Africa is linked to both insolation forcing and high-latitude climate variability. The δ^{13}C record indicates that vegetation of the western Sahel was consistently dominated by C_4 plants during the past 44 ka, whereas C_3-type vegetation increased during the Holocene. Moreover, we observe a gradual ending of the Holocene humid period together with unchanging ratio of C_3 to C_4 plants, indicating that an abrupt aridification due to vegetation feedbacks is not a general characteristic of this time interval.

1. Introduction

Tropical monsoon variability and associated rain belt migration is a prominent feature of global atmospheric circulation and the resulting heat distribution over the globe. As part of the global monsoon system, the West African monsoon has been linked to the precessional cycle of the Earth's orbit and related variability in insolation through associated changes in the land–ocean pressure gradient and sea-surface temperature (eg, Kutzbach, 1981; Rossignol-Strick, 1983; Pokras and Mix, 1987; Kutzbach and Liu, 1997). Internal non-linear responses such as vegetation–albedo feedbacks (eg, Charney, 1975; Kutzbach et al., 1996; Ganopolski et al., 1998) may induce abrupt climate shifts despite a gradual insolation forcing (eg, Claussen et al., 1999; deMenocal et al., 2000). The most recent wet phase of northwest Africa, the so-called African humid period (14.8–5.5 ka), occurred during a period of maximal summer insolation and is regarded as an example of the insolation-driven intensity of the West African monsoon (Gasse, 2000). Studies of marine records from the continental slope off West Africa by Weldeab et al. (2007) (Nigeria) and Tjallingii et al. (2008) (Mauritania) show a general correlation between the West African monsoon and insolation intensity, but also a decreased monsoonal response to insolation forcing during the last glacial period. This latter feature is attributed to a lower amplitude of insolation variability and increasing global ice sheet coverage. Other studies of marine cores collected from Senegal (Mulitza et al., 2008) and Mauritania (Jullien et al., 2007) also show sensitivity of northwest African climate to high-latitude climate variations

* Corresponding author. California Institute of Technology, Department of Geological and Planetary Sciences, 17 Mail Stop 100-23, Pasadena, CA 91125, USA. Tel.: +1 626 395 1785; fax: +1 626 683 0621.
E-mail addresses: eniedermeyer@caltech.edu, eniedermeyer@marum.de (E.M. Niedermeyer), schefuss@uni-bremen.de (E. Schefuß), als@gps.caltech.edu (A.L. Sessions), smulitza@uni-bremen.de (S. Mulitza), gesine.mollenhauer@awi.de (G. Mollenhauer), mschulz@uni-bremen.de (M. Schulz), gwefer@marum.de (G. Wefer).

0277-3791/$ – see front matter © 2010 Elsevier Ltd. All rights reserved.
doi:10.1016/j.quascirev.2010.06.039

during North Atlantic Heinrich stadials, indicating multiple controls on the West African monsoon. These stadials are less pronounced in the humidity index of Tjallingii et al. (2008) and are absent in estimates of the intensity of the West African monsoon inferred from fluvial runoff variation (Weldeab et al., 2007).

To provide a better understanding of long term variability of the West African monsoon, we used the stable hydrogen and carbon isotopic composition (δD and δ^{13}C) and abundance of terrestrial plant wax *n*-alkanes in a marine sediment core from the continental slope off Senegal as proxies for past changes in continental hydrology, vegetation composition and density. The δD values of plant waxes have been applied successfully in earlier studies, eg, on marine sediments off the Congo basin (Schefuß et al., 2005) and on lacustrine sediments from Lake Tanganyika (Tierney et al., 2008), revealing valuable insights into the controls of the central and southeast African monsoon.

Our data show that the West African monsoon over tropical northwest Africa is linked to both insolation forcing and high-latitude climate variability during the Younger Dryas and North Atlantic Heinrich stadials of the past 44 ka.

2. Study area

2.1. Core location

Marine sediment core GeoB9508-5 was retrieved during RV Meteor cruise M65/1 (Mulitza et al., 2006). The core location (15°29.90′N, 17°56.88′W) is ~160 km southwest of the Senegal River mouth on the continental slope off Senegal at 2384 m water depth (Fig. 1). The terrigenous fraction of continental slope sediments at this location is derived from both Senegal River suspended load and from aeolian dust (Sarnthein et al., 1981; Mulitza et al., 2008).

2.2. Environmental setting

Western Sahel precipitation derives from the Gulf of Guinea and, to a lesser extent, from the tropical Atlantic off northwest Africa (Gong and Eltahir, 1996). It is transported to the Sahel by the West African monsoon and is further recycled by cloud convective systems and evapotranspiration over the continent (Nicholson, 2009). The amount of rainfall in the Sahel (Fig. 2a) depends on the moisture content of the West African monsoon and the position of the tropical rain belt, moving between 10 and 20°N following seasonal changes in maximum solar insolation. As a result, total annual rainfall and duration of the rainy season decrease from the Guinea coast (>3000 mm yr^{-1}) to the Sahara desert (0–100 mm yr^{-1}) (compare Willmott and Matsuura database, http://climate.geog.udel.edu/~climate). Maximum precipitation over the Sahel (100–500 mm yr^{-1}) occurs during the northern hemisphere summer from July to September when the rain belt reaches its northernmost position, followed by a long dry season for the rest of the year when the rain belt moves southward. The north–south rainfall gradient is reflected by decreasing rainwater δD values (Fig. 2b) from the Sahara desert to 10°N (due to the amount effect (Dansgaard, 1964)) where they form a "bullseye", and increase again southward to the Guinea coast (reflecting the continental effect (Dansgaard, 1964)).

Following the seasonal migration of the rain belt and the associated rainfall gradient, vegetation (Fig. 1) gradually shifts from desert to dense tropical vegetation forming latitudinal bands oriented almost parallel to the equator (White, 1983). The Sahara desert is sparsely vegetated by few C_4 plants and to a negligible extent by CAM plants. The adjacent Sahel comprises both semi-desert grassland (100–250 mm yr^{-1}) dominated by C_4 grasses and herbs, and dry savannah (250–500 mm yr^{-1}) with sporadic C_3 trees. Due to its transitional nature, the Sahel is a sensitive ecosystem that is highly susceptible to even small climatic changes (Dupont, 1993).

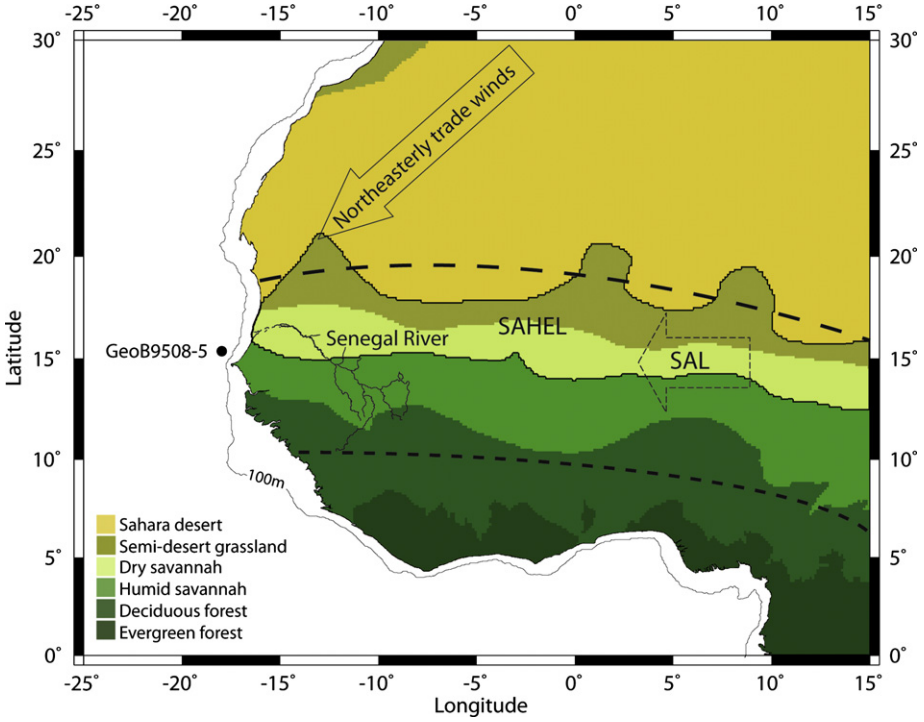

Fig. 1. Position of core GeoB9508-5 and vegetation zones of tropical Northwest Africa (after White, 1983). Upper (lower) dashed line indicates the approximate northernmost (southernmost) position of the tropical rain belt during northern hemisphere summer (winter). Arrows indicate dominant direction of northeasterly trade winds and the Saharan Air Layer (SAL).

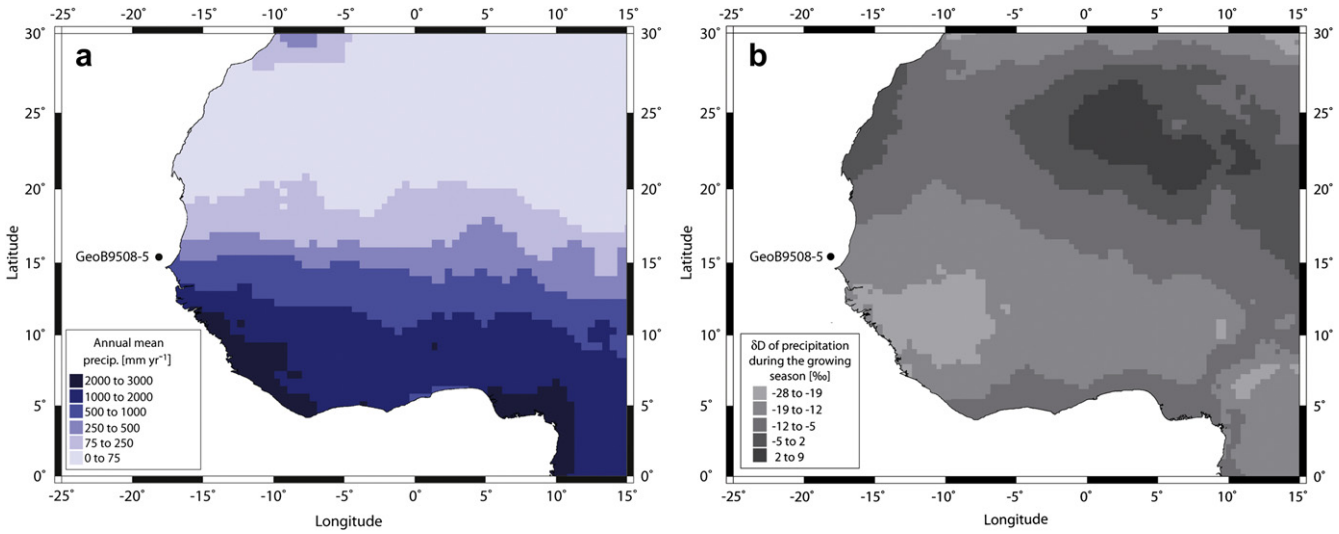

Fig. 2. (a) Mean annual rainfall over tropical northwest Africa. Graphic is based on a compilation of rainfall data from the period 1950–1999 available on the Willmott, Matsuura and Collaborators Global Resources Pages (http://climate.geog.udel.edu/~climate/), Center for Climatic Research at University of Delaware. (b) Stable hydrogen isotopic composition (δD) of precipitation over tropical northwest Africa during the growing season. Graphic is based on data from www.waterisotopes.org (Bowen and Revenaugh, 2003; Bowen, 2009).

It is bordered by the humid savannah (500–1000 mm yr^{-1}) which receives sufficient rainfall to maintain a higher vegetation cover consisting of both tall C_4 grasses and trees (C_3). It shifts to tropical deciduous forests (1000–2000 mm yr^{-1}) toward the equator that become evergreen forests (2000–3000 mm yr^{-1}; both dominated by C_3 plants) at the Guinea coast.

During the dry season, the northwest African continent is dominated by low-level ($\geq$900 hPa) northeastern trade winds (Sarnthein et al., 1981) (Fig. 1) that blow almost parallel to the West African coast. An additional wind system, the high-level atmospheric African Easterly Jet, is most intense during northern hemisphere summer and carries dust within the so-called Saharan Air Layer. Dust of the Saharan Air Layer originates from the southern Sahara and the Sahel, and is uplifted to higher atmospheric levels and deposited in the Atlantic between 10 and 25°N. These two regimes are the most important agents of aeolian plant wax transport (Huang et al., 2000) to the ocean off West Africa. However, due to the fine grain size and widespread distribution of dust in the Saharan Air Layer its contribution to sediments at the core location is relatively low compared to dust transported from more proximal regions by the northeastern trade winds (Stuut et al., 2005).

The study site also receives terrigenous material transported by the Senegal River (Sarnthein et al., 1981; Mulitza et al., 2008) located between ~11–16°N and 10–16°W with a total drainage area of approximately 350,000 km^2 (Fig. 1). Given the north–south precipitation gradient, the major portion of Senegal River discharge is generated in the tropical deciduous forests of the Guinea Mountains and southern Mali, whereas the contribution from higher tropical latitudes is small. Sedimentary discharge is closely related to water runoff (Gac and Kane, 1986) and thus is highest during the rainy season from June to October and drops to almost zero during the end of the dry season.

3. Methods

The age model of the core is based on a combination of radiocarbon dating and benthic stable oxygen isotope stratigraphy as described in detail by Mulitza et al. (2008). Briefly, 12 radiocarbon ages were measured on samples of planktonic foraminifera and corrected for a reservoir age of 400 years. ^{14}C ages smaller than 40 ka were converted to calendar ages (Fairbanks et al., 2005); seven additional age points were set by alignment of the core's benthic $\delta^{18}O$ record to the $\delta^{18}O$ stratigraphy of core MD95-2042 (Shackleton et al., 2004).

A total of 94 samples were collected from the upper 692 cm of the core at 4–20 cm intervals, resulting in an average temporal resolution of about 460 years.

3.1. Lipid extraction, identification and quantitation

Lipids were extracted from freeze-dried and finely ground sediment samples by ultrasonication in methanol (MeOH), 1:1 MeOH/dichloromethane (DCM), and DCM. An internal standard (squalane) was added to the total lipid extracts. Each total lipid extract was then washed with bi-distilled water (Seralpur) to remove salts, dried over anhydrous Na_2SO_4, and concentrated by rotary evaporation and under N_2. Next, total lipid extracts were saponified with 0.5 M KOH in MeOH at 80 °C for 3 h. Neutral lipids were extracted with hexane and separated by silica–gel column chromatography. Alkanes were eluted with hexane, then further purified by $AgNO_3$-silica gel column chromatography again using hexane as eluent.

n-Alkanes were identified by gas chromatography/flame ionization detector (GC/FID) by comparing their retention times to a standard mixture containing the corresponding *n*-alkanes at known concentrations. Alkane abundances were quantified using the FID peak areas calibrated against the standard mixture. Final *n*-alkane concentrations in the sediment were corrected for losses during sample preparation using the internal standard by assuming identical losses of standard and sample *n*-alkanes. Repeated analyses of a reference sediment yielded a mean precision of 0.2 μg g^{-1} for *n*-alkane abundance.

3.2. δD measurements

The δD values of individual *n*-alkanes were measured using a Thermo Trace GC^{ULTRA} coupled to a Thermo Finnigan $Delta^{+}XP$ isotope-ratio mass spectrometer via a pyrolysis furnace operated at 1430 °C. Data processing and the daily H_3^+ correction were accomplished using Isodat v2.5 software as described by Sessions et al. (2001). An external standard containing 15 homologous

n-alkanes (from C_{16} to C_{30}) with known δD values was analyzed repeatedly with the samples, and yielded a standard deviation (1σ) of 2.7‰ and root-mean-squared accuracy of 2.7‰. In addition, an internal standard (C_{36} *n*-alkane) was coinjected with all samples and yielded a standard deviation (1σ) of 1.8‰ with a mean deviation from the known δD value of 9‰. Due to a limited sample size, replicate analyses were not possible for every sample. Those that were analyzed in replicate yielded a mean standard deviation (1σ) of 2.3‰. All δD values are reported in permil [‰] relative to the V-SMOW standard.

3.3. $\delta^{13}C$ measurement

The $\delta^{13}C$ values of individual *n*-alkanes were measured using a Thermo Trace GC^{ULTRA} coupled to a Finnigan MAT 252 IRMS via a Finnigan GC/C III combustion interface operated at 960 °C. To monitor the system's performance, a standard mixture containing squalane and 16 homologous *n*-alkanes (C_{20}–C_{36}) with known $\delta^{13}C$ values was analyzed repeatedly. The $\delta^{13}C$ values of sample analytes were calibrated against CO_2 with known isotopic composition and the internal standard (squalane). Samples were analyzed in duplicate or triplicate with a standard deviation (1σ) for the *n*-C_{31} alkane of 0.5‰. Values of $\delta^{13}C$ are reported relative to the V-PDB standard.

4. Results

We report δD values only for the *n*-C_{31} alkane, which was the most cleanly separated compound of adequate abundance. Time series of the δD values of the *n*-C_{27} and *n*-C_{29} alkane (data not shown) exhibited the same overall pattern as the *n*-C_{31} alkane, indicating that the interpretation of our data is not biased by the leaf wax *n*-alkane chain length. The δD values of the *n*-C_{31} alkane (Fig. 3c, pink line) vary between −163 and −124‰. Values of δD corrected for ice volume changes (Fig. 3c, black line) are generally lower during the last glacial interval with a slightly smaller amplitude of variability between −167 and −133‰. The overall structure of both records exhibits a periodic pattern that is correlated with variations in intensity of local summer insolation at 15°N (Fig. 3d, insolation values are shown for July 21 after Berger (1978)). Lowest δD values are observed during periods of highest insolation between 38–28 ka and 15–4 ka, whereas periods of reduced insolation coincide with higher δD values. In order to analyze the δD record for variations other than those linked to the insolation pattern, we applied a high-pass filter (Rybicki and Press, 1995) with a cut-off frequency of 1/(10,000 yr). The filtered data (Fig. 4c) indicate an excursion toward higher values between 9 and 7 ka and further enrichments that coincide with the intervals of the Younger Dryas interval and Heinrich stadials (HS) 1, 3 and 4.

All HS intervals reflected in the δD record coincide with decreased plant wax *n*-alkane concentrations (Fig. 3a), which exhibit considerable variation between 1.7 and 0.4 μg g^{-1}. HS2, which is only weakly expressed in the δD record, can be clearly identified in the record of *n*-alkane concentration.

The $\delta^{13}C$ values of *n*-C_{31} alkane (Fig. 3b) vary between −26 and −21‰ and show no overall variation attributable to either insolation or HS. Generally, the $\delta^{13}C$ record varies between about −21 and −24‰ during the last glacial period and gradually decreases to −26‰ starting at around 18 ka. We used a two-component mixing calculation to estimate the contribution of *n*-C_{31} from C_4 plants by assuming $\delta^{13}C$ values of −21‰ and −36‰ for the C_4 and C_3 end members, respectively (Rieley et al., 1993; Collister et al., 1994). This calculation indicates a C_4 contribution of between 85 and 100% during the last glacial, and a gradual decrease to 75% toward the end of the record. During HS2 the $\delta^{13}C$ record indicates an increase of C_4 plant waxes up to 100%. This is the HS with the least variability in the δD record.

5. Discussion

5.1. Sources of long-chain sedimentary n-alkanes

Long-chain *n*-alkanes are integral parts of epicuticular waxes from vascular plant leaves (Eglinton and Hamilton, 1967). They have typical chain lengths ranging from C_{25} to C_{35} and exhibit a dominance of odd-carbon numbered over even-numbered homologues (Eglinton and Hamilton, 1967; Kolattukudy, 1976). The extent of this odd-over-even predominance can be quantified as the carbon preference index (CPI) with generally high values (>5) (eg, Collister et al., 1994) for *n*-alkanes from higher plant waxes. Long-chain *n*-alkanes that derive from other sources such as petroleum or that released from other carbon pools through diagenetic processes exhibit lower to negligible chain length predominance and have a low CPI (<1) (Kolattukudy, 1976). We report a range of CPI between 5.3 and 7.8 with an average CPI of 6.6 and a standard deviation (1σ) of 0.6 for *n*-alkanes at the study site indicating higher terrestrial plants as the major source throughout the entire record.

5.2. Provenance of sedimentary plant wax n-alkanes

The study site receives terrigenous sediment contributions from both aeolian dust and Senegal River suspended load (Sarnthein et al., 1981; Mulitza et al., 2008). Today, aeolian dust deposited at the study site is mainly carried by the northeastern trade winds (Stuut et al., 2005), whereas the Senegal River basin drains more humid areas to the south. Thus, the possibility must be considered that the plant waxes originate from different geographic sources and that the contribution of these sources may vary depending on climate. To date there are no studies examining the contribution of fluvial vs. aeolian derived plant waxes to sediments off northwest Africa. Pronounced fluvial input of plant wax *n*-alkanes should be indicated in the $\delta^{13}C$ record by enhanced contribution of C_3 derived *n*-alkanes during wet periods, because the Senegal River drains more humid areas with increasing C_3 vegetation toward the south. As will be described in more detail in the following section, this pattern is not observed suggesting that fluvial input of plant wax *n*-alkanes from its southern catchment to the study site is of minor importance compared to the input through aeolian dust. This agrees with studies of Lézine and Hooghiemstra (1990) indicating that very little fluvial pollen transport took place in the region even in front of the Senegal outlet. However, minor plant wax contributions from the northern catchment draining parts of the Sahel may still occur. In summary, we expect that the transport of plant waxes to the study site is mainly by aeolian dust (Huang et al., 2000; Schefuß et al., 2003). Plant waxes transported by the low-level northeastern trade winds (Schefuß et al., 2003) most likely represent the vegetation type underlying the final section of the air-mass trajectory (Simoneit et al., 1989; Schefuß et al., 2003) rather than the vegetation along the entire path. Because the northeastern trade winds blow almost parallel to the northwest African coast, plant waxes deposited at the study site are likely abraded from the vegetation of northern Senegal, southwestern Mauritania and western-central Mali and, therefore, reflect an integrated signal of the climatic conditions in these areas.

5.3. Controls on plant wax $\delta^{13}C$ variability

The $\delta^{13}C$ value of plant wax *n*-alkanes can be used to distinguish C_3-from C_4-type vegetation with the isotopic difference resulting from physiological differences during CO_2 acquisition for

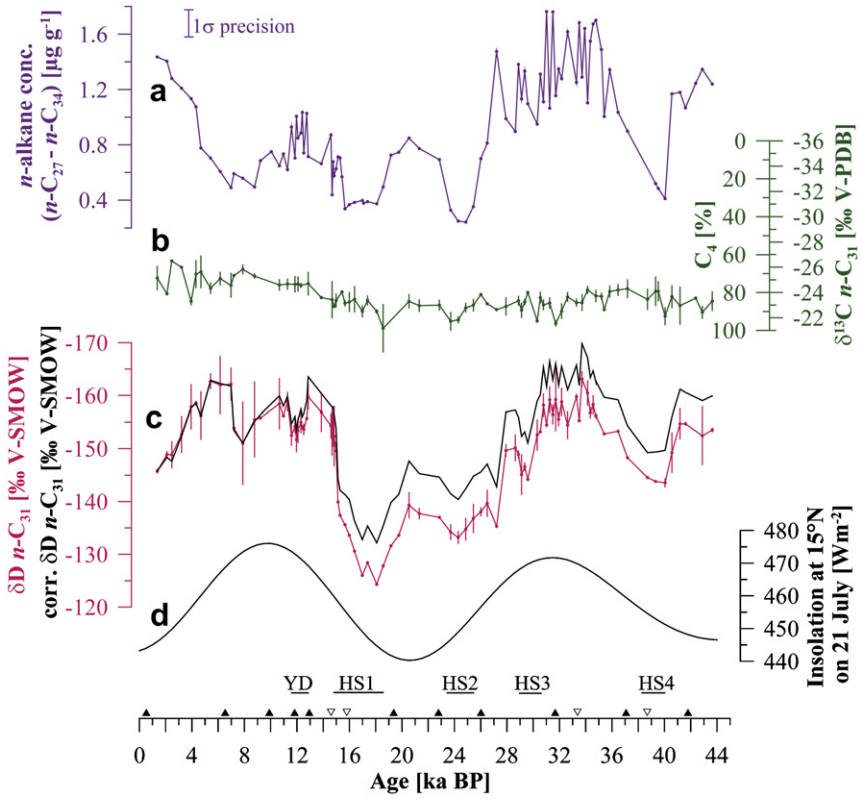

Fig. 3. Temporal evolution of (a) sedimentary *n*-alkane concentration; (b) stable carbon isotopic composition ($\delta^{13}C$) of the C_{31} *n*-alkane (right axis) and fractional contribution of C_4 vegetation (left axis); (c) pink line: stable hydrogen isotopic composition (δD) of the *n*-C_{31} alkane (*n*-C_{31}); (c) black line: δD of the *n*-C_{31} alkane corrected for ice volume effects; (d) insolation at 15°N on 21 July after Berger (1978). Filled triangles indicate age points derived by radiocarbon dating, open triangles indicate age points derived by correlation with the benthic $\delta^{18}O$ record of core MD95-2042 (Mulitza et al., 2008). Error bar in (a) reflects the average precision as deduced from the internal standard. Error bars (1σ) for (b) and (c) are given for multiple-measurement samples. Data points without error bars derive from single measurements. (For interpretation of the references to colour in this figure legend, the reader is referred to the web version of this article).

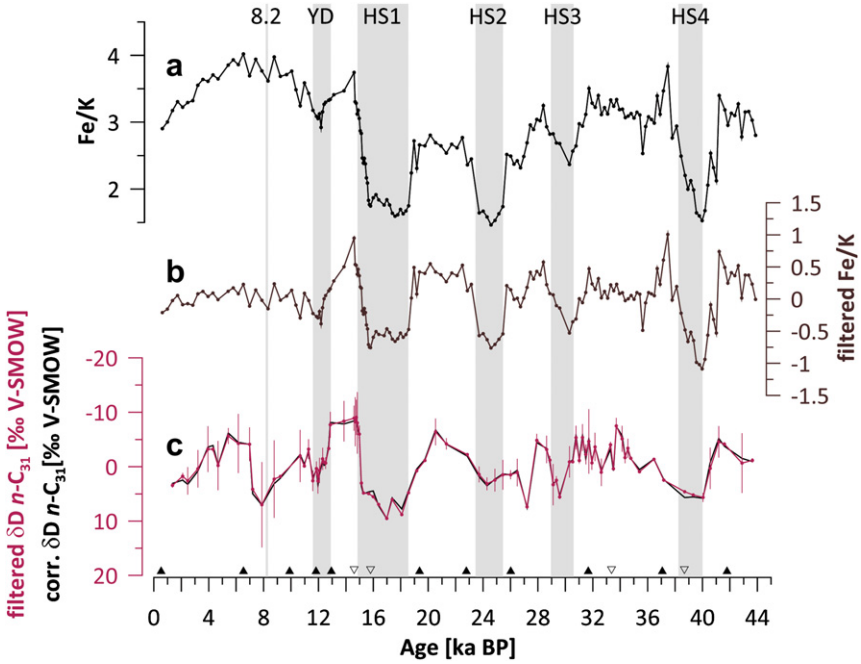

Fig. 4. Temporal variability of (a) the Fe/K record from the same core (Mulitza et al., 2008), (b) the Fe/K record and (c) the δD record both after high-pass filtering (Rybicki and Press, 1995) with a cut-off frequency of 1/(10,000 yr) to show variability other than linked to insolation. Gray bars indicate periods of Heinrich stadials (HS, after Sarnthein et al. (2001)), the Younger Dryas interval (YD) and the "8.2 ka" event. Filled triangles indicate age points derived by radiocarbon dating, open triangles indicate age points derived by correlation with the benthic $\delta^{18}O$ record of core MD95-2042 (Mulitza et al., 2008). Error bars (1σ) are given for multiple-measurements only.

photosynthesis (O'Leary, 1981). It varies between −21‰ (C_4 type) and −36‰ (C_3 type) (values are for the *n*-C_{31} alkane; Rieley et al., 1993; Collister et al., 1994). The range of atmospheric pCO_2 is much smaller (Indermühle et al., 1999), making the photosynthetic pathway the dominant control on the isotopic signature of plant waxes. The geographic distribution of C_3 and C_4 plants depends on climate parameters such as water availability, atmospheric CO_2, insolation intensity and temperature (Larcher, 2003). In tropical northwest Africa, C_4-type grasses and herbs are the dominant species of the semi-desert and savannah grasslands with increasing contribution of C_3-type species (mainly shrubs and trees) with increasing humidity toward the equator (White, 1983). The competitive advantage of C_4 over C_3 herbaceous plants in hot and arid environments such as northwest Africa is due to their ability to internally concentrate CO_2 prior to photosynthetic fixation. This allows for lower stomatal conductivity reducing the transpirational loss of water. The growing season of C_4 grasses is characterized by higher minimum temperatures and a shorter rainy season compared to that required for C_3 plants. In addition, low atmospheric pCO_2 may influence the dispersal of C_3 plants as a limiting factor of photosynthesis (Collatz et al., 1998; Bond et al., 2003; Larcher, 2003).

5.4. Controls on plant wax δD variability

Variability in the δD values of plant wax *n*-alkanes has been shown to relate to the δD-value of the plant source water (Sessions et al., 1999; Chikaraishi and Naraoka, 2003; Huang et al., 2004; Sachse et al., 2004, 2006; Hou et al., 2008). In high latitudes, the δD-value of rainwater is mainly a function of temperature driving progressive depletion of rainfall with decreasing temperature through Rayleigh distillation (Dansgaard, 1964; Rozanski et al., 1993; Alley and Cuffey, 2001). Therefore, ice core δD and $\delta^{18}O$ records obtained from polar latitudes have been applied as paleothermometers (eg, Grootes and Stuiver, 1997, Johnsen et al., 1997). In the tropics, however, this temperature effect is not generally detectable as shown in the study of Rozanski et al. (1993). This is because initial cloud formation (through tropical convergence) and precipitation are spatially close – a feature that can be assumed to have persisted over the time of our record – leading to a negligible impact of tropical temperature change on rainwater δD through progressive Rayleigh distillation. Instead, the dominant effect controlling precipitation δD over the study area is the "amount effect" (Dansgaard, 1964; Rozanski et al., 1993; Worden et al., 2007; Risi et al., 2008a,b) with rainfall intensity controlling re-evaporation (and as a consequence, isotopic enrichment) of the falling rain. This leads to lower values (that is stronger *D*-depletion through less re-evaporation) in areas of high precipitation and higher values (*D*-enrichment through more re-evaporation) when precipitation is low. Taken together, we expect that any potential influence of temperature on the isotopic composition of precipitation at the study site will be small compared to the amount effect. Provided that the local controls on the δD-value of precipitation are stable over time, changes in the isotopic composition of plant wax *n*-alkanes reflect changes in the amount of precipitation.

Strictly speaking it is not the isotopic composition of precipitation that is recorded by plant waxes but rather that of leaf water (eg, Pendall et al., 2005). This water source may be *D*-enriched relative to precipitation by soil evaporation and leaf transpiration (eg, Dongmann et al., 1974; Epstein et al., 1977; Flanagan et al., 1991), suggesting an additional influence of relative humidity on leaf wax δD. Such a link has been found in studies of recent lake-surface sediments along a north-south European transect (Sachse et al., 2004), in grasses from greenhouse and natural environments across the central USA (Smith and Freeman, 2006) and in shrubs and trees from semi-arid to arid regions of southern California (Feakins and Sessions, 2010). A survey of lake-surface sediments across a transect of southwestern USA by Hou et al. (2008), however, found no correlation between in situ source-water/leaf wax fractionation and relative humidity. The question of how much relative humidity influences *D*-enrichment in leaf waxes thus remains unresolved. Regardless, both effects (soil water evaporation, leaf water transpiration and the amount effect on precipitation) should point in the same climatic direction, causing *D*-enrichment of leaf waxes during more arid conditions (Worden et al., 2007).

There is also debate about whether vegetation type has an influence on leaf wax δD through differences in leaf anatomy, photosynthetic pathway or rooting depth (Chikaraishi and Naraoka, 2003; Liu et al., 2006; Smith and Freeman, 2006; Hou et al., 2007; Liu and Yang, 2008). Values of $\delta^{13}C$ for the *n*-C_{31} alkane in our record (Fig. 3b) do not vary considerably during the last glacial and show no correlation with the δD record, suggesting that plant type variability likely exerts little influence on the δD signal at the study site. Furthermore, the δD values of plant waxes extracted from surface sediments along a north–south European transect (Sachse et al., 2004) correlate well with the isotopic composition of the referring rainfall, indicating that species specific differences are smoothed in the integrated sedimentary signal.

Influence on plant wax δD other than West African monsoon intensity is exerted by ice volume effects on the δD-value of meteoric water. To account for this, the *n*-alkane δD record was corrected for glacial–interglacial changes in seawater isotopic composition as follows. The average global change in seawater $\delta^{18}O$ since the Last Glacial Maximum is about 1.0‰ (eg, Schrag et al., 2002; Waelbroeck et al., 2002). To account for additional seawater $\delta^{18}O$ variability prior to the Last Glacial Maximum, we corrected the *n*-alkane δD record using the benthic $\delta^{18}O$ record obtained from tests of *Cibicidoides wuellerstorfi* from the same core (Mulitza et al., 2008). The benthic $\delta^{18}O$ record was converted to the V-SMOW scale and adjusted to match the Last Glacial interglacial shift of 1‰ (set after Schrag et al. (2002) as the maximal amplitude of the $\delta^{18}O$ decrease between the Last Glacial Maximum and the Holocene). The equivalent δD variability was calculated using the global meteoric water line (Craig, 1961). This correction does not account for changes caused by variability of deuterium excess which comprises a range of ~4‰ within the past 45 ka (Masson-Delmotte et al., 2005). The corrected data (Fig. 3c, black line) account for an approximation of these effects and show lower δD values during the last glacial but no changes in the overall temporal structure.

Taken together, we interpret lower plant wax δD values in our record as reflecting periods of enhanced precipitation and/or higher humidity ('wetter'), though we cannot specifically disentangle those two effects. Similarly, higher δD values likely reflect intervals of drier conditions. In addition, since plant wax *n*-alkane production occurs during the growing season, we infer that δD variability likely corresponds to climatic variability during the growing (wet) season and, hence, to rainfall intensity during the rainy season. However, based on the δD record alone we cannot deduce West African monsoon variability relating to a shortening or expansion of the wet season.

5.5. Orbital-scale climate variability

The large-scale variability of both δD records (raw and ice-volume corrected, Fig. 3c) matches the temporal structure of variations in local summer insolation at 15°N (Fig. 3d), exhibiting two wetter periods between 38–28 and 15–4 ka that coincide with highest summer insolation. This suggests a link between insolation

variability and the West African monsoon. Indeed, such a link has been described by earlier studies (Wang et al., 2001; Yuan et al., 2004; Weldeab et al., 2007; Tjallingii et al., 2008) as a global feature of monsoon systems. However, Tjallingii et al. (2008) recently presented grain-size data from a marine core off Mauritania indicating a decreased influence of insolation on the West African monsoon during the last glacial period. They attribute their findings to the generally weaker amplitude of insolation variability during marine isotope stage 3 of the last glacial period in combination with an expansion of the northern hemisphere ice caps. This leads to an intensification of the dry northeastern trade winds that limits the northward extension of the West African monsoon. Our data, however, indicate that the current study site – which is located ~3° further south – was under the climatic influence of an insolation-forced West African monsoon during the last glacial period. This suggests that the border between the two wind systems may have been located between 17° and 20°N during this period.

The δD record indicates insolation forcing of the West African monsoon between 38 and 28 ka. Further evidence for this wet period from terrestrial archives (eg, lacustrine deposits) is sparse and equivocal, and faces the problem of erosion during dry intervals. In addition, lower sampling resolution in earlier terrestrial studies using marine archives (eg, Lézine and Casanova, 1991) further complicate comparison to our data. They indicate a preceding humid phase between 52 and 44 ka which unfortunately is not covered by our record. Regardless, a precession forced humid period between 38 and 28 ka is in agreement with earlier evidence for orbital controls on West African monsoon (Rossignol-Strick, 1983; Pokras and Mix, 1987; McIntyre et al., 1989; Collister et al., 1994; Gasse, 2000).

Although plant wax δD is a sensitive proxy for the isotopic composition of precipitation it is not yet possible to quantify the changes with respect to rainfall amounts. Judging from δD values alone, however, precipitation intensity throughout the rainy season during the last glacial wet period and the wet period during the Holocene might have been similar. However, the $\delta^{13}C$ record (Fig. 3b) does not show an increase of C_3 plants during the last glacial wet period (the proportion of about 90% C_4 plants remains almost constant), indicating that the length of the rainy season was not high enough to sustain significant C_3 vegetation. Today, in order to support a woodland–grass savannah (humid savannah) with considerable contribution of C_3 shrubs and trees, rainfall in northwest Africa must exceed 400 mm $year^{-1}$ (Walter, 1970). From this, one might infer that rainfall over the source area during the last glacial wet period was below 400 mm $year^{-1}$. Low atmospheric pCO_2 during the last glacial period (Indermühle et al., 2000) may have further stabilized the dominance of C_4 plants (Collatz et al., 1998; Bond et al., 2003). Continuously high sedimentary *n*-alkane concentrations (Fig. 3a), in spite of lower wind intensity and aeolian dust supply during this period (Jullien et al., 2007), point to increased terrestrial biomass possibly related to an increase in C_4 plant abundance. However, changes in plant wax availability can be caused by both, vegetation density and plant wax availability (e.g., cuticle thickness). Furthermore, sediment *n*-alkane concentration may vary with dust flux intensity (dilution effect) (compare Adkins et al., 2006). Taken together, we suppose that mean annual precipitation between 38 and 28 ka was lower than during the Holocene humid period, which is in agreement with earlier studies (eg, Gasse, 2000) pointing to generally drier conditions during the last glacial. However, rainfall intensities during the rainy season were presumably similar during both wet periods.

The second wet period identified within the δD record reaches its maximum from 15 to 4 ka. This agrees with earlier studies that describe an insolation-forced African humid period during the Holocene (eg, deMenocal et al., 2000; Gasse, 2000; Salzmann et al., 2002). In contrast to the study by deMenocal et al. (2000) we do not observe an abrupt end of the African humid period but a rather gradual decrease of precipitation starting around 5 ka. Vegetation type (the ratio of C_3 to C_4 plants) also shows no abrupt changes in response to the decrease in precipitation, the $\delta^{13}C$ signal remains rather stable. However, we note that different hydrologic preferences within a photosynthetic pathway exist and that changes in vegetation composition toward drier conditions may have occurred without notable changes in vegetation type ($\delta^{13}C$).

deMenocal et al. (2000) attribute the abruptness to non-linear vegetation and albedo feedbacks (Charney, 1975; Kutzbach, 1981; Kutzbach et al., 1996). For this to occur, vegetation cover needs to fall below a certain threshold to produce an abrupt non-linear response to the gradual orbital forcing (Claussen et al., 1999). The gradual decrease observed within this study agrees with compilation studies of pollen data (Lézine, 2009; Watrin et al., 2009) and observations of Mulitza et al. (2008) from the same core as well as with studies from the Lake Tilla crater (northeastern Nigeria) (Salzmann et al., 2002) and Lake Yoa (northern Chad) (Kröpelin et al., 2008). Thus, an abrupt termination about 5.5 ka is not a general characteristic of the Holocene African humid period, possibly because vegetation density at some locations did not fall below the threshold value required for an abrupt climate transition.

Interestingly, palynological analyses indicate an abrupt vegetation shift toward modern semi-arid conditions in Senegal around 2 ka (eg, Lézine, 1988, 1989) which is about 3.5 ka later than observed by deMenocal et al. (2000) indicating that the Holocene humid period was shorter in the North and longer in the South. Unfortunately, the time interval between 2 and 1 ka (the end of our record) is covered by only two data points and so does not allow for further comparison at this time. We further note that several abrupt changes occurring at different times in different regions may appear smoothened in the integrated δD record.

5.6. Millennial-scale climate variability

The high-pass filtered δD record (Fig. 4b) reveals climate forcing of arid intervals other than those linked to insolation. Millennial-scale dry periods coincide with North Atlantic Heinrich stadials (HS) in agreement with other studies from near Senegal (Mulitza et al., 2008; Itambi et al., 2009) and Mauritania (Jullien et al., 2007). Whereas most of the proxies applied in these studies likely reflect enhanced dust input during the dry season, we ascribe *D*/*H* variability of plant wax *n*-alkanes to climatic conditions during the wet season. Our data, therefore, indicate that climate variability during HS also affected the rainy season toward drier conditions. In order to depict the distinct responses of the wet and dry seasons, we show Fe/K ratios from the same core (Fig. 4a) (Mulitza et al., 2008) using the same high-pass filtering (Fig. 4b) as for the δD record. Lower Fe/K ratios correspond to decreased riverine input and enhanced dust supply, suggesting drier conditions during these intervals (Mulitza et al., 2008).

HS2 seems to be anomalous in its weak response (if at all) in the δD record. Sedimentary *n*-alkanes (Fig. 3a), in contrast, show a pronounced decrease in abundance. This may derive from both lowered plant wax production and increased dust input (as reconstructed by Jullien et al. (2007)) and points toward intensification of the dry season. Fe/K ratios in sediments from the same core (Fig. 4a, b) (Mulitza et al., 2008) also indicate intensification of the dry season during HS2. The δD record, however, exhibits only slight variation during this period, whereas the $\delta^{13}C$ values (Fig. 3b) suggest an increase in C_4 plant abundance. We speculate that this could reflect a shortening of the rainy season without a concomitant change in precipitation rate. This would lead to an extended

dry season favoring C_4 plants over trees but with little change in precipitation δD values during the growing season.

The filtered data indicate additional aridification between 13 and 11.5 ka. Such a drying event has been widely observed in tropical Northwest Africa, eg, in lacustrine sediments from Lake Tilla (northeastern Nigeria) (Salzmann et al., 2002), Lake Bosumtwi (Ghana) (Talbot and Johannessen, 1992; Peck et al., 2004; Shanahan et al., 2006) and Lake Barombi Mbo (western Cameroon) (Maley and Brenac, 1998), and is attributable to the Younger Dryas interval.

The δD record indicates a further excursion toward dry conditions between 9 and 7 ka. The data for this period have large error bars, complicating the interpretation. However, aridification of tropical African climate within this interval is reported in a range of studies (eg, Gasse and Van Campo, 1994; Gasse, 2000; Shanahan et al., 2008) which supports the persistence of drier conditions in the western Sahel around 8 ka as indicated by the δD record. This interval possibly coincides with the "8.2 ka" event, a period of colder conditions in the high-latitude North Atlantic realm and beyond (Alley et al., 1997; Alley and Ágústsdóttir, 2005; Ellison et al., 2006).

The dry episodes during Heinrich stadials, the Younger Dryas interval and around the 8.2 ka event coincide with reduced Atlantic overturning circulation (McManus et al., 2004; Ellison et al., 2006) and are probably induced by cool North Atlantic sea-surface temperatures (Mulitza et al., 2008; Niedermeyer et al., 2009). In the model of Mulitza et al. (2008), an abrupt drop in extratropical northeast Atlantic sea-surface temperature creates a positive sea level pressure anomaly over northern North Africa. This leads to a southward shift of the monsoon trough, with the Sahel drying further being amplified by an intensification of the African Easterly Jet. The intervals of lowered precipitation identified within the δD record indicate that this mechanism is important for tropical West African climate throughout the seasons.

6. Conclusions

The pattern of δD variability in terrestrial leaf wax *n*-alkanes suggests persistent local insolation forcing of the West African monsoon during the past 44 ka. We identify two wet periods from 38 to 28 ka and from 15 to 4 ka that coincide with maximal local summer insolation. Rainfall intensity during the growing season was presumably similar throughout both wet periods, whereas mean annual precipitation was lower between 38 and 28 ka than during the Holocene humid period.

Millennial-scale intervals of reduced precipitation/humidity are identified that coincide with North Atlantic Heinrich stadials 1, (2), 3 and 4, the Younger Dryas interval and, possibly, the "8.2 ka" event. We, therefore, conclude that the West African monsoon is susceptible to both local insolation and North Atlantic climate. This suggests a crucial role of the North Atlantic in controlling tropical northwest African climate.

We observe a gradual end of the Holocene African humid period in the western Sahel which implies that decreasing precipitation did not initiate non-linear vegetation feedbacks as suggested for an abrupt climate transition during this period. The ratio of C_3 to C_4 plants at the study site generally shows low correlation to changes in hydrology indicating that additional controls such as atmospheric pCO_2 may have been relevant during the period covered by this record.

Acknowledgements

This work was funded by the German Science Foundation (DFG) through the Research Center/Excellence Cluster "The Ocean in the Earth System" at MARUM – Center for Marine Environmental Sciences, University of Bremen and by the U.S. National Science Foundation grant EAR-0645502 to ALS. ES is funded through DFG grant Sche 903/8. EMN acknowledges additional support by GLOMAR – Bremen International Graduate School for Marine Sciences. We thank the captain and crew of RV Meteor cruise M65/1 during which core GeoB9508-5 was collected. The German academic exchange service (DAAD) is acknowledged for funding a research stay at Caltech. We are grateful to Lydie Dupont for thorough comments on the manuscript and thank Jan-Berend Stuut (MARUM) for providing information on the provenance of aeolian dust at the study site. We thank an anonymous reviewer for comments that helped to improve the manuscript. Martin Erbs (Bundesforschungsinsitut Braunschweig) is acknowledged for helpful discussions on the ecology of plants.

References

Adkins, J., DeMenocal, P.B., Eshel, G., 2006. The "African humid period" and the record of marine upwelling from excess ^{230}Th in Ocean Drilling Program Hole 658C. Paleoceanography 21.

Alley, R.B., Ágústsdóttir, A.M., 2005. The 8 k event: cause and consequences of a major Holocene abrupt climate change. Quat. Sci. Rev. 24, 1123–1149.

Alley, R.B., Cuffey, K.M., 2001. Oxygen- and hydrogen-isotopic ratios of water in precipitation: beyond paleothermometry. In: Valley, J.W., Cole, D.R. (Eds.), Stable Isotope Geochemistry. Mineralogical Society of America & Geochemical Society.

Alley, R.B., Mayewski, P.A., Sowers, T., Stuiver, M., Taylor, K.C., Clark, P.U., 1997. Holocene climatic instability: a prominent, widespread event 8200 year ago. Geology 25, 483–486.

Berger, A.L., 1978. Long-term variations of daily insolation and Quaternary climatic changes. J. Atmos. Sci. 35, 2362–2367.

Bond, W.J., Midgley, G.F., Woodward, F.I., 2003. The importance of low atmospheric CO_2 and fire in promoting the spread of grasslands and savannas. Glob. Change Biol. 9, 973–982.

Bowen, G.J., 2009. Gridded maps of the isotopic composition of meteoric precipitation. http://www.waterisotopes.org.

Bowen, G.J., Revenaugh, J., 2003. Interpolating the isotopic composition of modern meteoric precipitation. Water Resour. Res. 39, 1299.

Charney, J.G., 1975. Dynamics of deserts and drought in the Sahel. Q.J.R. Meteorol. Soc. 101, 193–202.

Chikaraishi, Y., Naraoka, H., 2003. Compound-specific δD-δ^{13}C analyses of *n*-alkanes extracted from terrestrial and aquatic plants. Phytochemistry 63, 361–371.

Claussen, M., Kubatzki, C., Brovkin, V., Ganopolski, A., Hoelzmann, P., Pachur, H.-J., 1999. Simulation of an abrupt change in Saharan vegetation in the mid-Holocene. Geophys. Res. Lett. 26, 2037–2040.

Collatz, G.J., Berry, J.A., Clark, J.S., 1998. Effects of climate and atmospheric CO_2 partial pressure on the global distribution of C_4 grasses: present, past, and future. Oecologia 114, 441–454.

Collister, J.W., Rieley, G., Stern, B., Eglinton, G., Brian, F., 1994. Compound-specific δ^{13}C analyses of leaf lipids from plants with differing carbon dioxide metabolism. Org. Geochem. 21, 619–627.

Craig, H., 1961. Isotopic variations in meteoric waters. Science 133, 1702–1703.

Dansgaard, W., 1964. Stable Isotopes in Precipitation, vol. 16. Tellus, Sweden. p. 436–468.

deMenocal, P.B., Ortiz, J., Guilderson, T., Adkins, J., Sarnthein, M., Baker, L., Yarusinsky, M., 2000. Abrupt onset and termination of the African humid period: rapid climate response to gradual insolation forcing. Quat. Sci. Rev. 19, 347–361.

Dongmann, G., Nürnberg, H.W., Förstel, H., Wagener, K., 1974. On the enrichment of $H_2^{18}O$ in the leaves of transpiring plants. Radiat. Environ. Biophys. 11, 41–52.

Dupont, L.M., 1993. Vegetation zones in NW Africa during the brunhes chron reconstructed from marine palynological data. Quat. Sci. Rev. 12, 189–202.

Eglinton, G., Hamilton, R.J., 1967. Leaf epicuticular waxes. Science 156, 1322–1335.

Ellison, C.R.W., Chapman, M.R., Hall, I.R., 2006. Surface and deep ocean interactions during the cold climate event 8200 years ago. Science 312, 1929–1932.

Epstein, S., Thompson, P., Yapp, C.J., 1977. Oxygen and hydrogen isotopic ratios in plant cellulose. Science 198, 1209–1215.

Fairbanks, R.G., Mortlock, R.A., Chiu, T.-C., Cao, L., Kaplan, A., Guilderson, T.P., Fairbanks, T.W., Bloom, A.L., Grootes, P.M., Nadeau, M.-J., 2005. Radiocarbon calibration curve spanning 0 to 50,000 years BP based on paired 230Th/234U/238U and 14C dates on pristine corals. Quat. Sci. Rev. 24, 1781–1796.

Feakins, S.J., Sessions, A.L., 2010. Controls on the *D*/*H* ratios of plant leaf waxes in an arid ecosystem. Geochim. Cosmochim. Acta. 74, 2128–2141.

Flanagan, L.B., Bain, J.F., Ehleringer, J.R., 1991. Stable oxygen and hydrogen isotope composition of leaf water in C_3 and C_4 plant species under field conditions. Oecologia 88, 394–400.

Gac, J.-Y., Kane, A., 1986. Le fleuve Sénégal: I. Bilan hydrologique et flux continentaux de matières particulaires a l'embouchure. Sci. Géol. Bull. 39, 99–130.

Ganopolski, A., Kubatzki, C., Claussen, M., Brovkin, V., Petoukhov, V., 1998. The influence of vegetation–atmosphere–ocean interaction on climate during the mid-Holocene. Science 280, 1916–1919.

Gasse, F., 2000. Hydrological changes in the African tropics since the Last Glacial Maximum. Quat. Sci. Rev. 19, 189–211.
Gasse, F., Van Campo, E., 1994. Abrupt post-glacial climate events in West Asia and North Africa monsoon domains. Earth. Planet. Sci. Lett. 126, 435–456.
Gong, C., Eltahir, E., 1996. Sources of moisture for rainfall in West Africa. Water. Resour. Res. 32, 3115–3121.
Grootes, P.M., Stuiver, M., 1997. Oxygen 18/16 variability in Greenland snow and ice with 10-3 to 105-year time resolution. J. Geophys. Res. 102, 26455–26470.
Hou, J., D'Andrea, W.J., Huang, Y., 2008. Can sedimentary leaf waxes record *D*/*H* ratios of continental precipitation? Field, model, and experimental assessments. Geochim. Cosmochim. Acta. 72, 3503–3517.
Hou, J., D'Andrea, W.J., MacDonald, D., Huang, Y., 2007. Hydrogen isotopic variability in leaf waxes among terrestrial and aquatic plants around Blood Pond, Massachusetts (USA). Org. Geochem. 38, 977–984.
Huang, Y., Dupont, L., Sarnthein, M., Hayes, J.M., Eglinton, G., 2000. Mapping of C_4 plant input from north West Africa into north East Atlantic sediments. Geochim. Cosmochim. Acta. 64, 3505–3513.
Huang, Y., Shuman, B., Wang, Y., Webb, T., 2004. Hydrogen isotope ratios of individual lipids in lake sediments as novel tracers of climatic and environmental change: a surface sediment test. J. Paleolimnol. 31, 363–375.
Indermühle, A., Monnin, E., Stauffer, B., Stocker, T.F., Wahlen, M., 2000. Atmospheric CO_2 concentration from 60 to 20 kyr BP from the Taylor Dome ice core, Antarctica. Geophys. Res. Lett. 27, 735–738.
Indermühle, A., Stocker, T.F., Joos, F., Fischer, H., Smith, H.J., Wahlen, M., Deck, B., Mastroianni, D., Tschumi, J., Blunier, T., Meyer, R., Stauffer, B., 1999. Holocene carbon-cycle dynamics based on CO_2 trapped in ice at Taylor Dome, Antarctica. Nature 398, 121–126.
Itambi, A.C., Von Dobeneck, T., Mulitza, S., Bickert, T., Heslop, D., 2009. Millennial-scale northwest African droughts related to Heinrich events and Dansgaard–Oeschger cycles: evidence in marine sediments from offshore Senegal. Paleoceanography 24.
Johnsen, S.J., Clausen, H.B., Dansgaard, W., Gundestrup, N.S., Hammer, C.U., Andersen, U., Andersen, K.K., Hvidberg, C.S., Dahl-Jensen, D., Steffensen, J.P., Shoji, H., SveinbjörnsdóttirÁ.E., White, J., Jouzel, J., Fishe, D., 1997. The δ18O record along the Greenland Ice Core Project deep ice core and the problem of possible Eemian climatic instability. J. Geophys. Res. 102, 26397–26410.
Jullien, E., Grousset, F., Malaize, B., Duprat, J., Sánchez-Goni, M.-F., Eynaud, F., Charlier, K., Schneider, R., Bory, A., Bout, V., Flores, J.A., 2007. Low-latitude "dusty events" vs. high latitude "icy Heinrich events". Quat. Res. 68, 379–386.
Kolattukudy, P.E., 1976. Chemistry and Biochemistry of Natural Waxes. Elsevier Scientific Pub. Co., Amsterdam, New York.
Kröpelin, S., Verschuren, D., Lézine, A.-M., Eggermont, H., Cocquyt, C., Francus, P., Cazet, J.-P., Fagot, M., Rumes, B., Russel, J.M., Darius, F., Conley, D.J., Schuster, M., von Suchodoletz, H., Engstrom, D.R., 2008. Climate-driven ecosystem succession in the Sahara: the past 6000 years. Science 320, 765–768.
Kutzbach, J., Bonan, G., Foley, J., Harrison, S.P., 1996. Vegetation and soil feedbacks on the response of the African monsoon to orbital forcing in the early to middle Holocene. Nature 384, 623–626.
Kutzbach, J.E., 1981. Monsoon climate of the early Holocene: climate experiment with the earth's orbital parameters for 9000 years ago. Science 214, 59–61.
Kutzbach, J.E., Liu, Z., 1997. Response of the African monsoon to orbital forcing and ocean feedbacks in the middle Holocene. Science 278, 440–443.
Larcher, W., 2003. Physiological Plant Ecology: Ecophysiology and Stress Physiology of Functional Groups. Springer.
Lézine, A.-M., 1989. Late quaternary vegetation and climate of the Sahel. Quat. Res. 32, 317–334.
Lézine, A.-M., 2009. Timing of vegetation changes at the end of the Holocene Humid Period in desert areas at the northern edge of the Atlantic and Indian monsoon systems. Compt. Rend. Geosci. 341, 750–759.
Lézine, A.-M., Casanova, J., 1991. Correlated oceanic and continental records demonstrate past climate and hydrology of North Africa (0–140 ka). Geology 19, 307–310.
Lézine, A.M., 1988. New pollen data from the Sahel, Senegal. Rev. Palaeobot. Palynol. 55, 141–154.
Lézine, A.M., Hooghiemstra, H., 1990. Land–sea comparisons during the last glacial–interglacial transition: pollen records from West Tropical Africa. Palaeogeogr. Palaeoclimatol. Palaeoecol. 79, 313–331.
Liu, W., Yang, H., 2008. Multiple controls for the variability of hydrogen isotopic compositions in higher plant *n*-alkanes from modern ecosystems. Glob. Change Biol. 14, 2166–2177.
Liu, W., Yang, H., Li, L., 2006. Hydrogen isotopic compositions of *n*-alkanes from terrestrial plants correlate with their ecological life forms. Oecologia 150, 330–338.
Maley, J., Brenac, P., 1998. Vegetation dynamics, palaeoenvironments and climatic changes in the forests of western Cameroon during the last 28,000 years B.P. Rev. Palaeobot. Palynol. 99, 157–187.
Masson-Delmotte, V., Jouzel, J., Landais, A., Stievenard, M., Johnsen, S.J., White, J.W.C., Werner, M., Sveinbjornsdottir, A., Fuhrer, K., 2005. GRIP deuterium excess reveals rapid and orbital-scale changes in Greenland moisture origin. Science 309, 118–121.
McIntyre, A., Ruddiman, W.F., Karlin, K., Mix, A.C., 1989. Surface water response of the equatorial Atlantic Ocean to orbital forcing. Paleoceanography 4, 19–55.
McManus, J.F., Francois, R., Gherardi, J.M., Keigwin, L.D., Brown-Leger, S., 2004. Collapse and rapid resumption of Atlantic meridional circulation linked to deglacial climate changes. Nature 428, 834–837.
Mulitza, S., Bouimetarhan, I., Brüning, M., Freesemann, A., Gussone, N., Filipsson, H., Heil, G., Hessler, S., Jaeschke, A., Johnstone, H., Klann, M., Klein, F., Küster, K., März, C., McGregor, H., Minning, M., Müller, H., Ochsenhirt, W.-T., Paul, A., Schewe, F., Schulz, M., Steinlöchner, J., Stuut, J.-B., Tjallingii, R., von Dobeneck, T., Wiesmaier, S., Zabel, M., Zonneveld, K., 2006. Report and Preliminary Results of METEOR Cruise M65/1, Dakar-Dakar, 11.06–1.07.2005, Berichte, Fachbereich Geowissenschaften, Universität Bremen. University of Bremen, Bremen, p. 151.
Mulitza, S., Prange, M., Stuut, J.-B., Zabel, M., von Dobeneck, T., Itambi, A.C., Nizou, J., Schulz, M., Wefer, G., 2008. Sahel megadroughts triggered by glacial slowdowns of Atlantic meridional overturning. Paleoceanography 23.
Nicholson, S., 2009. A revised picture of the structure of the "monsoon" and land ITCZ over West Africa. Clim. Dynam. 32, 1155–1171.
Niedermeyer, E.M., Prange, M., Mulitza, S., Mollenhauer, G., Schefuß, E., Schulz, M., 2009. Extratropical forcing of Sahel aridity during Heinrich Stadials. Geophys. Res. Lett. 36.
O'Leary, M.H., 1981. Carbon isotopic fractionation in plants. Phytochemistry 20, 553–567.
Peck, J.A., Green, R.R., Shanahan, T., King, J.W., Overpeck, J.T., Scholz, C.A., 2004. A magnetic mineral record of Late Quaternary tropical climate variability from Lake Bosumtwi, Ghana. Palaeogeogr. Palaeoclimatol. Palaeoecol. 215, 37–57.
Pendall, E., Williams, D., Leavitt, S., 2005. Comparison of measured and modeled variations in piñon pine leaf water isotopic enrichment across a summer moisture gradient. Oecologia 145, 605–618.
Pokras, E.M., Mix, A.C., 1987. Earth's precession cycle and quaternary climatic change in tropical Africa. Nature 326, 486–487.
Rieley, G., Collister, J.W., Stern, B., Eglinton, G., 1993. Gas chromatography/isotope ratio mass spectrometry of leaf wax *n*-alkanes from plants of differing carbon dioxide metabolism. Rapid. Commun. Mass. Spectrom. 7, 488–491.
Risi, C., Bony, S., Vimeux, F., 2008a. Influence of convective processes on the isotopic composition (δ^{18}O and δD) of precipitation and water vapor in the tropics: 2. Physical interpretation of the amount effect. J. Geophys. Res. 113.
Risi, C., Bony, S., Vimeux, F., Descroix, L., Ibrahim, B., Lebreton, E., Mamadou, I., Sultan, B., 2008b. What controls the isotopic composition of the African monsoon precipitation? Insights from event-based precipitation collected during the 2006 AMMA field campaign. Geophys. Res. Lett. 35.
Rossignol-Strick, M., 1983. African monsoons, an immediate climate response to orbital insolation. Nature 304, 46–49.
Rozanski, K., Araguas-Araguas, L., Gonfiantini, R., 1993. Isotopic patterns in modern global precipitation. In: Climate Change in Continental Isotopic Records, Geophysical Monograph. American Geophysical Union, Washington DC p. 781–36.
Rybicki, G.B., Press, W.H., 1995. Class of fast methods for processing irregularly sampled or otherwise inhomogeneous one-dimensional data. Phys. Rev. Lett. Am. Phys. Soc., 1060.
Sachse, D., Radke, J., Gleixner, G., 2004. Hydrogen isotope ratios of recent lacustrine sedimentary *n*-alkanes record modern climate variability. Geochim. Cosmochim. Acta. 68, 4877–4889.
Sachse, D., Radke, J., Gleixner, G., 2006. δD values of individual *n*-alkanes from terrestrial plants along a climatic gradient – implications for the sedimentary biomarker record. Org. Geochem. 37, 469–483.
Salzmann, U., Hoelzmann, P., Morczinek, I., 2002. Late quaternary climate and vegetation of the Sudanian zone of Northeast Nigeria. Quat. Res. 58, 73–83.
Sarnthein, M., Stattegger, K., Dreger, D., Erlenkeuser, H., Grootes, P., Haupt, B., Jung, S., Kiefer, T., Kuhnt, W., Pflaumann, U., Schäfer-Neth, C., Schulz, H., Schulz, M., Seidov, D., Simstich, J., van Kreveld, S., Vogelsang, E., Völker, A., Weinelt, M., 2001. Fundamental modes and abrupt changes in North Atlantic circulation over the last 60 ky – concepts, reconstruction and numerical modeling. In: Schäfer, P., Ritzrau, W., Schlüter, M., Thiede, J. (Eds.), The Northern North Atlantic: A Changing Environment. Springer, Berlin, pp. 365–410.
Sarnthein, M., Tetzlaff, G., Koopmann, B., Wolter, K., Pflaumann, U., 1981. Glacial and interglacial wind regimes over the eastern subtropical Atlantic and North-West Africa. Nature, 193–196.
Schefuß, E., Ratmeyer, V., Stuut, J.-B.W., Jansen, J.H.F., Sinnighe Damsté, J.S., 2003. Carbon isotope analyses of *n*-alkanes in dust from the lower atmosphere over the central eastern Atlantic. Geochim. Cosmochim. Acta. 67, 1757–1767.
Schefuß, E., Schouten, S., Schneider, R.R., 2005. Climatic controls on central African hydrology during the past 20,000 years. Nature 437, 1003–1006.
Schrag, D.P., Adkins, J.F., McIntyre, K., Alexander, J.L., Hodell, D.A., Charles, C.D., McManus, J.F., 2002. The oxygen isotopic composition of seawater during the Last Glacial Maximum. Quat. Sci. Rev. 21, 331–342.
Sessions, A.L., Burgoyne, T.W., Hayes, J.M., 2001. Correction of H^{3+} contributions in hydrogen isotope ratio monitoring mass spectrometry. Anal. Chem. 73, 192–199.
Sessions, A.L., Burgoyne, T.W., Schimmelmann, A., Hayes, J.M., 1999. Fractionation of hydrogen isotopes in lipid biosynthesis. Org. Geochem. 30, 1193–1200.
Shackleton, N.J., Fairbanks, R.G., Chiu, T.-C., Parrenin, F., 2004. Absolute calibration of the Greenland time scale: implications for Antarctic time scales and for Δ14C. Quat. Sci. Rev. 1513–1522.
Shanahan, T.M., Overpeck, J.T., Scholz, C.A., Beck, J.W., Peck, J., King, J.W., 2008. Abrupt changes in the water balance of tropical west Africa during the late Quaternary. J. Geophys. Res. 113.
Shanahan, T.M., Overpeck, J.T., Wheeler, C.W., Beck, J.W., Pigati, J.S., Talbot, M.R., Scholz, C.A., Peck, J., King, J.W., 2006. Paleoclimatic variations in West Africa from a record of late Pleistocene and Holocene lake level stands of Lake Bosumtwi, Ghana. Palaeogeogr. Palaeoclimatol. Palaeoecol. 242, 287–302.

Simoneit, B.R.T., Cox, R.E., Standley, L.J., 1989. Organic matter of the troposphere–IV. Lipids in harmattan aerosols of Nigeria. Atmos. Environ., 983–1004.
Smith, F.A., Freeman, K.H., 2006. Influence of physiology and climate on δD of leaf wax *n*-alkanes from C_3 and C_4 grasses. Geochim. Cosmochim. Acta. 70, 1172–1187.
Stuut, J.-B., Zabel, M., Ratmeyer, V., Helmke, P., Schefuß, E., Lavik, G., Schneider, R., 2005. Provenance of present-day eolian dust collected off NW Africa. J. Geophys. Res. 110.
Talbot, M.R., Johannessen, T., 1992. A high resolution palaeoclimatic record for the last 27,500 years in tropical West Africa from the carbon and nitrogen isotopic composition of lacustrine organic matter. Earth. Planet. Sci. Lett. 110, 23–37.
Tierney, J.E., Russell, J.M., Huang, Y., Damste, J.S.S., Hopmans, E.C., Cohen, A.S., 2008. Northern hemisphere controls on tropical Southeast African climate during the past 60,000 years. Science, 252–255.
Tjallingii, R., Claussen, M., Stuut, J.-B.W., Fohlmeister, J., Jahn, A., Bickert, T., Lamy, F., Röhl, U., 2008. Coherent high- and low-latitude control of the northwest African hydrological balance. Nat. Geosci 1, 670–675.
Waelbroeck, C., Labeyrie, L., Michel, E., Duplessy, J.C., McManus, J.F., Lambeck, K., Balbon, E., Labracherie, M., 2002. Sea-level and deep water temperature changes derived from benthic foraminifera isotopic records. Quat. Sci. Rev. 21, 295–305.
Walter, H., 1970. Klimatisch Bedingte Savannen. Gräser und Holzarten als Antagonisten, Vegetationszonen und Klima. Ulmer, Stuttgart.
Wang, Y.J., Cheng, H., Edwards, R.L., An, Z.S., Wu, J.Y., Shen, C.C., Dorale, J.A., 2001. A high-resolution absolute-dated late Pleistocene monsoon record from Hulu Cave, China. Science 294, 2345–2348.
Watrin, J., Lézine, A.-M., Hély, C., 2009. Plant migration and plant communities at the time of the "green Sahara. Compt. Rend. Geosci. 341, 656–670.
Weldeab, S., Lea, D.W., Schneider, R.R., Andersen, N., 2007. 155,000 years of west African monsoon and ocean thermal evolution. Science 316, 1303–1307.
White, F., 1983. The Vegetation of Africa, Natural Resources Research. UNESCO, Paris.
Worden, J., Noone, D., Bowman, K., 2007. Importance of rain evaporation and continental convection in the tropical water cycle. Nature 445, 528–532.
Yuan, D., Cheng, H., Edwards, R.L., Dykoski, C.A., Kelly, M.J., Zhang, M., Qing, J., Lin, Y., Wang, Y., Wu, J., Dorale, J.A., An, Z., Cai, Y., 2004. Timing, duration, and transitions of the Last Interglacial Asian monsoon. Science 304, 575–578.